EXPERIMENTAL STUDY OF FLOW ABOUT A STALLED TWO-DIMENSIONAL AIRFOIL

National Aeronautics and Space Administration

Grant NGL 05-002-229

2nd, 3rd Semi-Annual Status Report

June, December 1972

(submitted January 1973)

D. Coles

A. Wadcock

B. Cantwell

California Institute of Technology

(NASA-CR-130919) EXPERIMENTAL STUDY OF FLOW ABOUT A STALLED TWO-DIMENSIONAL AIRFOIL Semiannual Status Report, Jun. - Dec. 1972 (California Inst. of Tech.) 25 p HC $3.25 CSCL 01C G3/02

N73-18020

Unclas 17168

Summary

The concept of using a ring wing to study flow about a stalled aerofoil has been abandoned in favor of using a plane wing. For the one ring configuration tested, the mean flow was found to be either non-symmetric or non-steady, depending on the method used to support the model. Furthermore, there was not a sufficiently extensive region of potential core flow to permit any hope that the ideas of thin aerofoil theory might eventually be extended to the stalled regime using these data.

1. DESIGN CONSIDERATIONS.

A. Facilities. The object of using a ring wing to study the separated region on a stalled aerofoil was to eliminate end effects by eliminating the ends. The research contemplates eventual use of a wing of 1.5 meter chord at a free-stream velocity of 50 m/sec, giving a Reynolds number of about 5×10^6. Because the cost of a ring model on this scale would be substantial, a small model was first commissioned to determine the suitability of the ring configuration.

Two facilities were available to test the small model; the Merrill wind tunnel (nominally 135 cm x 75 cm, with a maximum speed of 65 m/sec), and the free-surface water tunnel (50 cm x 50 cm, with a maximum speed of 7 m/sec). Both had advantages. The water tunnel offered easy alignment of the model in pitch and yaw and the use of dye or bubble injection for flow visualization, whereas the Merrill tunnel was more suitable for pressure surveys in the wake and for surface flow visualization by means of oil or paint.

B. Aerofoil Section. A well-documented aerofoil section possessing "good" stall characteristics was required (i.e., smooth $C_L - \alpha$ curve without sudden loss of lift at stall). For such sections, maximum lift is normally associated with trailing-edge separation occurring close to the 50-percent chord position. Inasmuch as Olson of NASA Ames Laboratory has recently begun a related investigation on a plane wing of section NACA 64_1-612, the same profile was chosen for the small ring wing. Olson's data suggest that the desired flow is achieved for a section incidence of 15° (see also NACA TN 1945, by Loftin & Smith, for tabulated aerofoil geometry and section properties in the Re range 0.7×10^6 to 9×10^6).

C. Model Geometry and Scale. By operating the Merrill wind tunnel at maximum speed, a Reynolds number of 10^6 is obtained for a model chord of 20 cm. To achieve the same Reynolds number in water with a chord of 20 cm requires a free-stream velocity of 5 m/sec, well within the capability of the free-surface water tunnel. A larger chord would increase the Reynolds number, the scale of the instrumentation, and the cost of the model. Hence 20 cm was chosen as a reasonable compromise for the chord.

For a given chord, the radius of the ring should be as large as practical so that locally two-dimensional conditions are approached on the wing. However, the diameter of the ring is restricted by the size of the working section of the free-surface water tunnel (the smaller of the two facilities). In choosing the ring radius a choice also had to be made between geometries with inside and outside stall, as shown below:

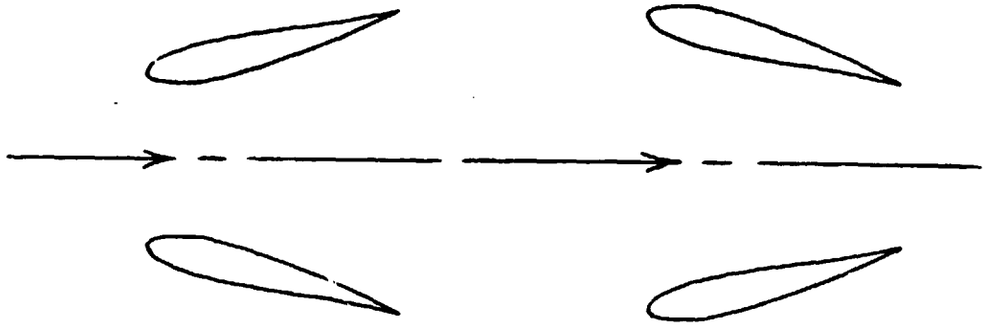

A. Inside Stall B. Outside Stall

The method of support plays a role in the choice of configuration. Presumably the model should be supported from the non-separating face to minimize interference, and this is more easily accomplished in the case of inside stall (configuration A). This configuration is

presumably also less sensitive to any interaction with the tunnel boundary layer. (The possibility of separation of the tunnel boundary layers is very real for both configurations, as the fluid flow outside the ring encounters an adverse pressure gradient in the vicinity of the model trailing edge.) Assuming that the model should be kept well away from the tunnel walls, and considering the size of the free-surface water tunnel working section, the diameter of the ring was also set at 20 cm. The two sketches above are drawn to scale.

Note that model B resembles a convergent nozzle. The entrance-to-exit ratio is approximately 4:1, implying a pressure coefficient approaching -15 at the trailing edge. It seems unlikely that the resulting pressure distribution would resemble the normal pressure distribution (see Olson's data in Figure 7 below). Moreover, for operation in the water tunnel at 5 m/sec, the exit velocity from the ring is large enough so that cavitation may occur at the trailing edge (which is thin and easily damaged) before it occurs at the nose.

Olson's pressure measurements indicate separation near the 50-percent chord position. For the inside-stall configuration A, separation may occur a little earlier because of an exaggerated adverse pressure gradient inside the ring (and also because of the lower Reynolds number). Hence, for separation occurring inside the ring, the 4:1 increase in geometric area is not fully effective. Thus the velocity outside the separated region but inside the ring may be only slightly different from that which would be encountered with a plane geometry, and the surface pressure coefficient on the model may be only slightly different from that found by Olson.

Configuration A has several disadvantages. Qualitative study of the separated region using flow-visualization techniques (such as bubble techniques in water) and quantitative measurements using laser-doppler techniques are both ruled out unless the model is transparent. The resemblance of the flow through the ring to that through a wide-angle diffuser also raises a distinct possibility that the flow separation may be non-uniform or non-symmetric.

In terms of accessibility with the whirling arm, the two configurations are rated nearly equal.

On balance, configuration A with inside stall seemed preferable and was chosen for the model test.

II. EXPERIMENTAL ARRANGEMENT.

A. Overall Program. Total-head pressure measurements in the wake were first scheduled for the Merrill wind tunnel to determine the degree of symmetry of separation obtainable with the ring wing. Static-pressure measurements and surface-flow visualization using oil were also planned. Further research, if indicated, would then be carried out in the free-surface water tunnel using a strain-gauge balance and using dye injection and other means of flow visualization. No surface pressure measurements were planned at this stage.

B. Model Installation. The 135 cm x 75 cm Merrill tunnel is of closed-return type, with a top speed of around 65 m/sec and a relatively high free-stream turbulence level of one percent. Plate 1 shows the ring-wing model supported from the roof of the working section by means of a single streamlined strut (flow is from left to right). The ring wing was machined from a solid block of

aluminium alloy and was anodized to obtain a matte black surface suitable for surface-flow visualization. The wing has a chord of 20 cm. The profile is the NACA 64_1-612 section at a geometric incidence of 15 degrees. The trailing-edge diameter of the ring is 22.3 cm. The slightly tapered support strut has a chord of about 14 cm and a maximum thickness of 1.9 cm and conceals a single 0.64-cm diameter stainless-steel bolt which supports the model. Two steel braces of section 1.27 cm x 0.16 cm, inclined at 45° to the support strut, were found to be necessary to reduce model vibration.

C. Instrumentation. Plate 1 also shows the streamlined vertical support strut for the wake-traverse mechanism. The pitot comb shown is mounted on a rotating sting which is aligned with the ring axis. The sting is rotated by a stepping motor and reduction gear box driving right-angle bevel gears. The sting and driving mechanism can be positioned axially over a distance of about two chord lengths. The stepping motor made 200 steps per revolution, each step being accompanied by an advancement of paper by 0.005 inches through a Houston Omnigraphic Model 6540 X-Y recorder. Pressures were measured by a Barocel Model 1083 electronic manometer which has both a digital display and an analog output. The latter signal was fed to the Y axis of the Omnigraphic recorder and/or to a Vidar Model 240 voltage-to-frequency converter and counter to obtain an average reading. For all of the recordings made on the Omnigraphic recorder the paper speed was two inches per minute, a value chosen by observing wake traverses behind the

support strut. Each trace required 5 minutes.

D. Procedure. The main investigation was carried out at a Reynolds number of 690,000 based on the model chord. It was found to be impractical to operate at the larger Reynolds number originally planned, due to overheating of the tunnel motor (no cooling vanes are installed in the Merrill wind tunnel at present). However, the high free-stream turbulence level may have compensated somewhat for the lower speed.

With the model supported from a single strut, as shown in Plate 1, total-head measurements in the wake were made at various radii using individual tubes of the pitot comb. These measurements were recorded as continuous traces on the Omnigraphic recorder. Two axial stations were chosen for the recordings; one close to the ring trailing edge, at x = 3.9 cm, and one farther downstream, at x = 24.3 cm (x is measured downstream from the trailing edge).

E. Initial Results for the Wake. With the wing supported from a single strut at zero incidence, pitot traverses in the wake at various radii showed that the total head was certainly not constant at constant radius. A typical record is shown in Figure 1. Note that the trace is well-defined, with only small fluctuations present. The polar plot of Figure 2a is derived from many such traces at different radii. For this configuration, the potential core is evidently deflected away from the support strut and toward the bottom of the ring. A similar picture is obtained farther downstream, as shown in Figure 2b, although the velocity gradients are now much smaller as expected.

Another anomaly in Figure 2 is that the wake seems to be skewed through a counter-clockwise angle of about 10^{o}. The flow quality in the tunnel is questionable, and the possibility of swirl cannot be ruled out. Unfortunately, the recording system did not allow data to be recorded with the probe moving in the reverse direction at the same speed in order to resolve this question.

F. Modifications to the Support Strut. In an effort to improve the symmetry of the flow, a dummy strut was added below the model, as shown in Plate 2. This second strut carries no load. The end in contact with the model is felt-covered and the strut is bolted to the tunnel floor in such a way as to ensure a close fit with the model surface.

With the dummy strut installed, the total head was found to be considerably more uniform, but the size of the fluctuations was greatly increased. This effect is shown in Figure 3, which is at the same axial station and radius as Figure 1. The equivalent polar plots of total head in the wake, shown in Figure 4, are somewhat less well-defined than for the case of a single strut, especially close to the trailing edge of the ring. The low-frequency fluctuations had a period of a few seconds (corresponding to one circuit period for the tunnel?), and the time taken to record each trace was five minutes. Filtering of the fluctuations would have increased this time by an order of magnitude and would have been completely impractical. Figure 4a does not therefore warrant close attention. However, farther downstream such large fluctuations were not present on the recorded traces, and the wake shown in Figure 4b is better defined.

The effect of adding the dummy strut is most apparent from a comparison of Figures 2a and 4a, at x = 3.9 cm. First, the isobars are much closer to being circular when the dummy strut is present. Second, the small potential core that was present when the model was supported from a single strut has now completely disappeared, probably as a result of the appearance of large low-frequency fluctuations.

G. Flow around a Yawed Ring Aerofoil. To test the usefulness of the ring configuration for generating smooth three-dimensional boundary-layer flow, the model was supported from a single strut and similar total-head measurements in the wake were made with the ring wing pitched 5° nose-up. This meant that the top section of the ring was at a geometric incidence of 10°, whereas the bottom section was at 20°. The corresponding polar plots are shown in Figure 5. The flow was quite steady. It seems likely that a ring model of somewhat higher aspect ratio and lower design angle of attack would be a quite satisfactory configuration for a study of three-dimensional separation.

H. Further Results with the Dummy Support Strut. Finally, the ring was returned to zero incidence, the dummy strut was re-installed, and the pitot comb was removed and replaced by a pitot-static tube. Preliminary static-pressure traces in the wake showed very little variation with angular position around the ring. Moreover, static pressures in a horizontal plane through the axis of the ring showed much smaller fluctuations than elsewhere in the flow. Separate pitot- and static-pressure measurements were therefore made over one

horizontal half-plane, inside the ring as well as outside, using the Vidar and counter to obtain steady mean data.

Total- and static-pressure measurements along the axis of the ring are presented in Figure 6 (for the static pressure, the quantity plotted is the pressure coefficient; for the total pressure the quantity plotted is normalized total pressure). Note that the total head on the axis begins to decrease even before the exit is reached. Note also that the total head does not appear to have begun its recovery to the free-stream value even one chord-length downstream. The measured static-pressure plot shows the expected decrease in pressure associated with the minimum in the area of the flow passage, followed by a plateau which corresponds to the separated region, and then by a gradual pressure recovery farther downstream.

Figure 7 shows a comparison of estimated surface static pressure, as extrapolated from measurements made inside the ring, with Olson's data for the same aerofoil section at the same 15-degree angle of attack.

Finally, Figure 8 shows some observations of the flow field associated with the ring wing as inferred from total- and static-pressure measurements in the half-plane described earlier. From the pitot-static measurements at the throat of the ring the mass flow through the ring can be calculated. Hence the radius at infinity (upstream and downstream) of the stream tube of fluid that passes through the ring is known. Assuming axial symmetry, the continuity equation and the measured streamwise velocity at various stations can be used to find the dividing streamline $\Psi = 0$. The individual

measurements of total and static pressure also yield the locus of points where the mean velocity vanishes. This locus is shown in Figure 8. These results are uncertain on two counts, and should be treated as qualitative at best. First, there is a serious doubt as to how much weight should be attached to readings of a pitot tube in a flow where the fluctuations in velocity are of the order of the mean velocity itself. Second, the assumption of axial symmetry for the experimental velocity distribution is demonstrably wrong in certain regions of the flow.

To the extent that the measurements are accepted as valid, the separation bubble is found to extend a considerable distance downstream - perhaps as much as half a chord. The separation point is slightly ahead of the 50-percent chord position. The upper boundary of the separation bubble, as defined by the streamline $\Psi = 0$, appears to be initially straight and nearly parallel to the flow at infinity, at least upstream of the trailing edge.

III. CONCLUSIONS.

A. Problems with the Ring Geometry. The initial attraction of the ring configuration was the possibility of achieving uniform separation around the ring, with a close approach to two-dimensional mean flow (in the axi-symmetric sense). In practice, use of a single support strut resulted in an unsymmetrical and hence unsatisfactory flow. With two struts the flow became more symmetrical, but large-amplitude, low-frequency fluctuations appeared. The cause of these fluctuations in unknown. It is possible that the model strut configuration is modifying the diffuser flow in the tunnel,

producing intermittent separation under some conditions. In any event, a strong impression was gained from this research that steady mean flow and axially symmetric mean flow are mutually antipathetic states.

An equally important defect is the absence of a potential core for the flow through the ring. If the results of the present research are eventually to be applied to analytical modelling of flow about stalled aerofoils, it seems essential for the experimental flow to have such a potential core at the trailing edge and for some distance downstream.

B. A Point of View. The success of thin aerofoil theory depends in two respects on the existence of potential flow everywhere except in a thin boundary layer and wake. First, far from the body, integration of the momentum equation about a large contour leads to the equivalence $L = \rho U \Gamma$, where L is the lift per unit span, U is the free-stream velocity, and Γ is the strength of the bound vorticity which represents the effect of the lifting aerofoil at large distances. Second, near the body, the aerofoil must be a streamline of the combined flow made up of a uniform stream, a suitably distributed potential vortex, and whatever source-sink distribution is appropriate for the shape in question. Provided that this shape has a sharp trailing edge, the Kutta-Joukowski condition can be used to remove the trailing-edge singularity for the combined flow. The result is a relation between the velocity in the uniform stream, the aerofoil geometry (thickness, camber, angle of attack), and the circulation. For the simplest case

of a flat plate, for example, this relation is $\Gamma = \pi\alpha Uc$, where α is the angle of attack and c is the chord. Elimination of Γ then gives $L = 2\pi\alpha(\rho U^2/2)c$, from which $C_L = 2\pi\alpha$.

The experimental evidence in Figure 8 suggests a point of view for the separated flow which may be capable of development to a useful state. If the aerofoil and the separation bubble together are thought of as a composite aerofoil (except that the bubble cannot support a pressure difference and in this sense does not contribute directly to the lift), the effects of separation and stall include the following:

a) The effective chord of the section increases;

b) the effective angle of attack decreases;

c) a reflex camber appears, corresponding to the observed stable or nose-down pitching moment at stall.

What remains is the difficult problem of preserving some modified form of the Kutta-Joukowsky condition in the stalled regime. In any event, the presence of an ambient potential flow is certainly desirable and probably essential.

C. Present Strategy. The results so far obtained for the ring wing show that the pressure rise downstream of the trailing edge of the ring, shown in Figure 6, is accompanied by an unexpectedly large increase in the rate of turbulence propagation toward the axis. The flow about the present ring is almost like the flow about a bluff body having a moderate amount of base bleed. To meet the requirement of providing a substantial potential core for the ring configuration, the ring diameter/chord ratio clearly would have to be increased; at the same time, the chord Reynolds number would have to be decreased. How much is not known, and can only be determined at this stage by

testing other models. For this and other reasons, the ring configuration has geen abandoned in favor of the more conventional plane wing. Some positive factors are:

a) A plane wing is much cheaper to construct, although additional effort is required for flow control near the ends;

b) the angle of attack of the aerofoil section need not be frozen at the design stage of the plane wing;

c) surface flow visualization on a plane wing is inherently less difficult;

d) the flying hot wire becomes much simpler, as it no longer needs to have a variable radius arm to enable it to pass inside the ring (motor-driven ballscrew and telescoping streamlined tubing are now redundant).

e) On the negative side, the advantage of the circular cross-section of the GLACIT 10-foot diameter wind tunnel is lost.

Finally, instrumentation problems with the full-scale wing (installation of pressure taps, thin-film gauges, proximity sensors, etc) have led to a decision to use a different aerofoil section with a more comfortable contour near the trailing edge. A good choice seems to be the NACA 4412 section, which is well documented in NACA Reports 563 and 613 by R. M. Pinkerton.

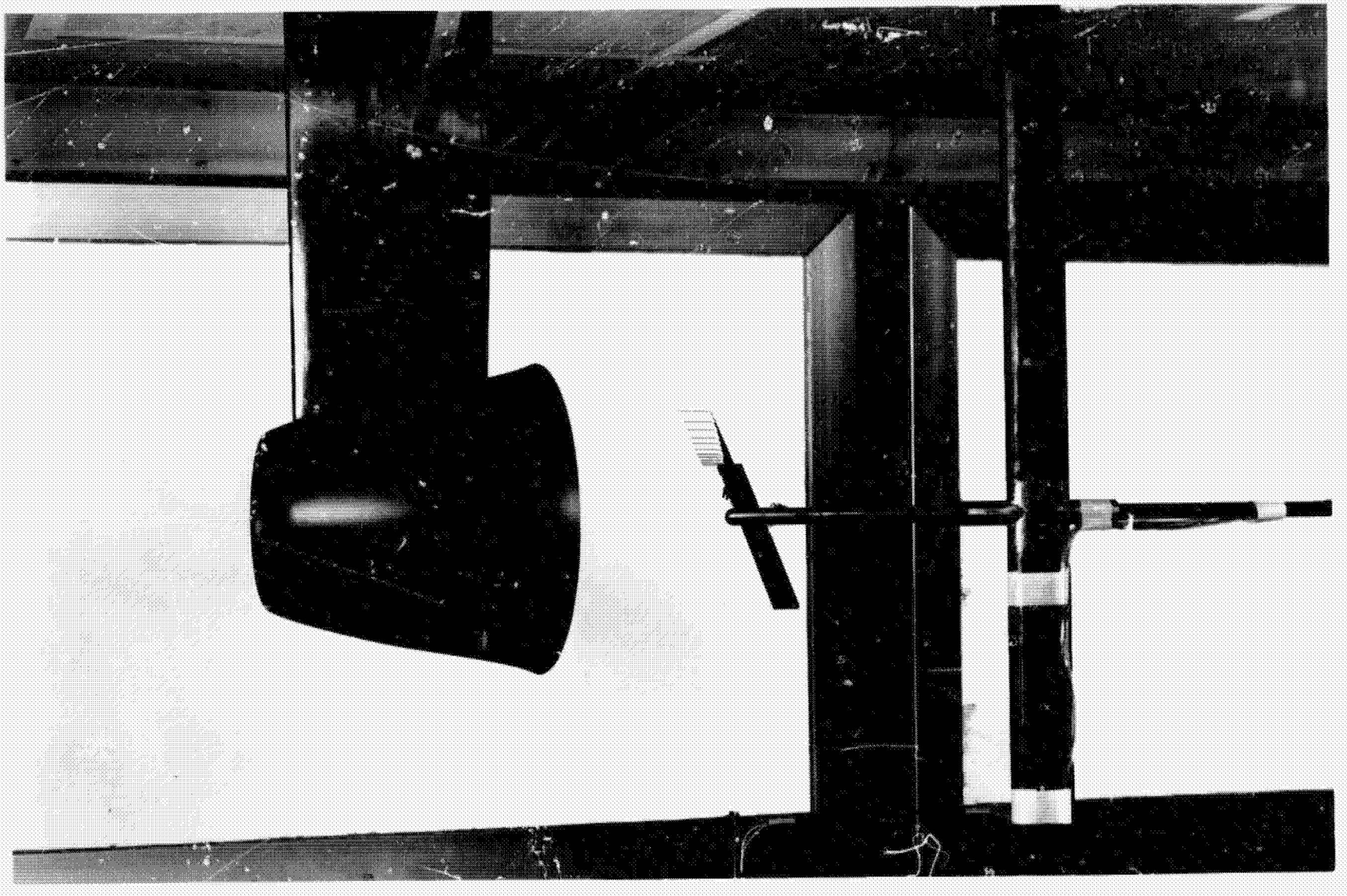

Plate 1. Ring Wing with
Single Support Strut

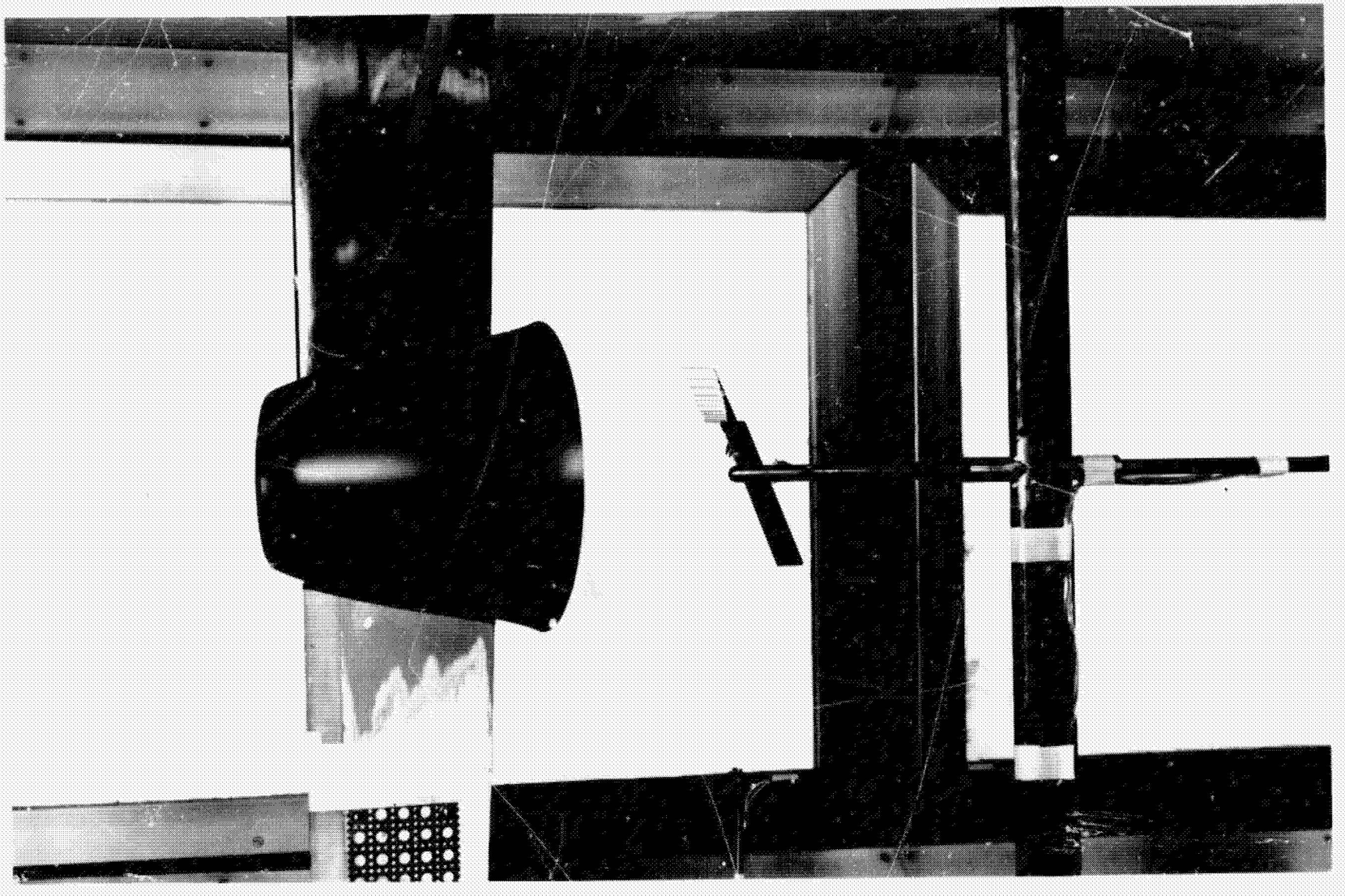

Plate 2. Ring Wing with
Dummy Strut Installed

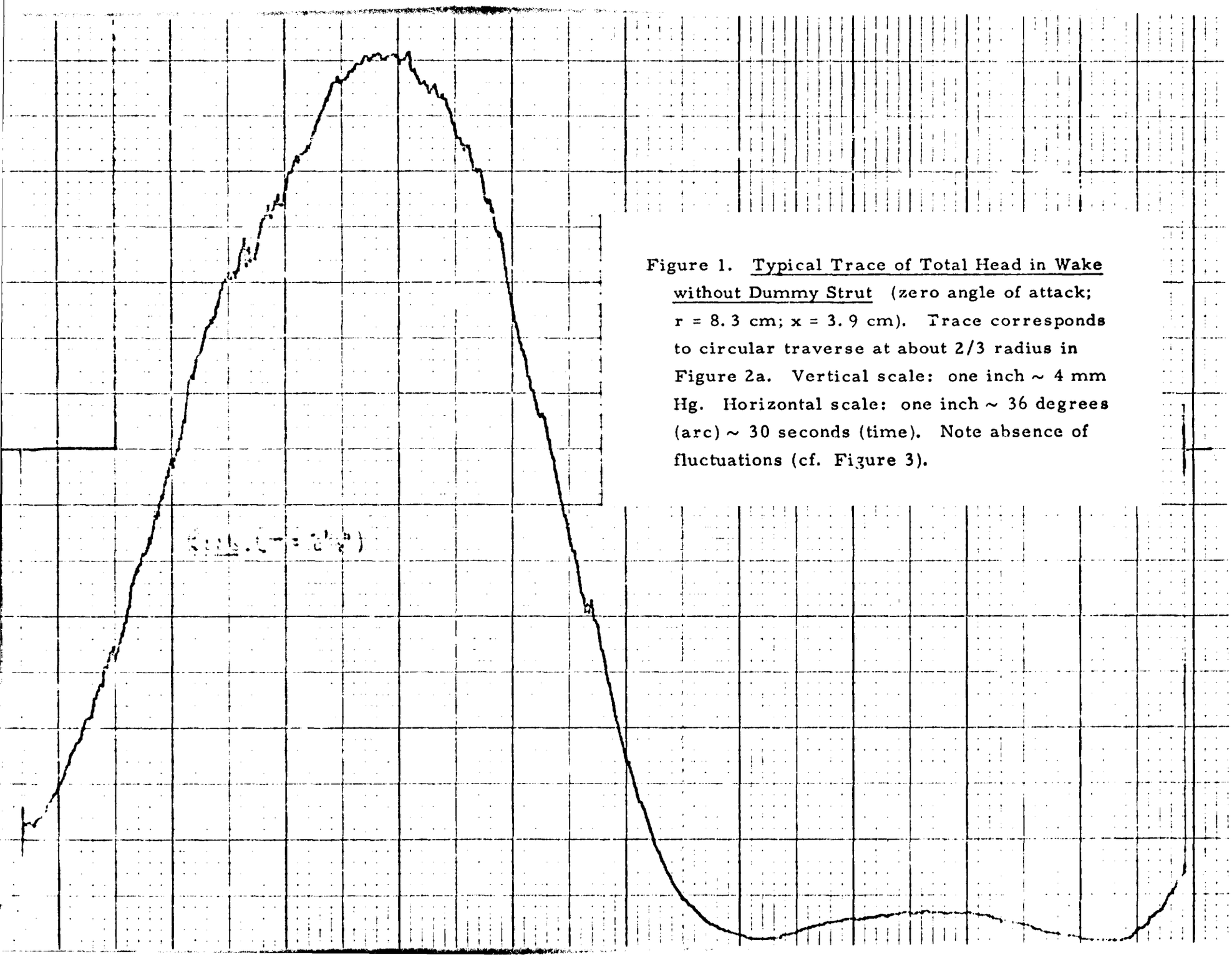

Figure 1. Typical Trace of Total Head in Wake without Dummy Strut (zero angle of attack; r = 8.3 cm; x = 3.9 cm). Trace corresponds to circular traverse at about 2/3 radius in Figure 2a. Vertical scale: one inch ~ 4 mm Hg. Horizontal scale: one inch ~ 36 degrees (arc) ~ 30 seconds (time). Note absence of fluctuations (cf. Figure 3).

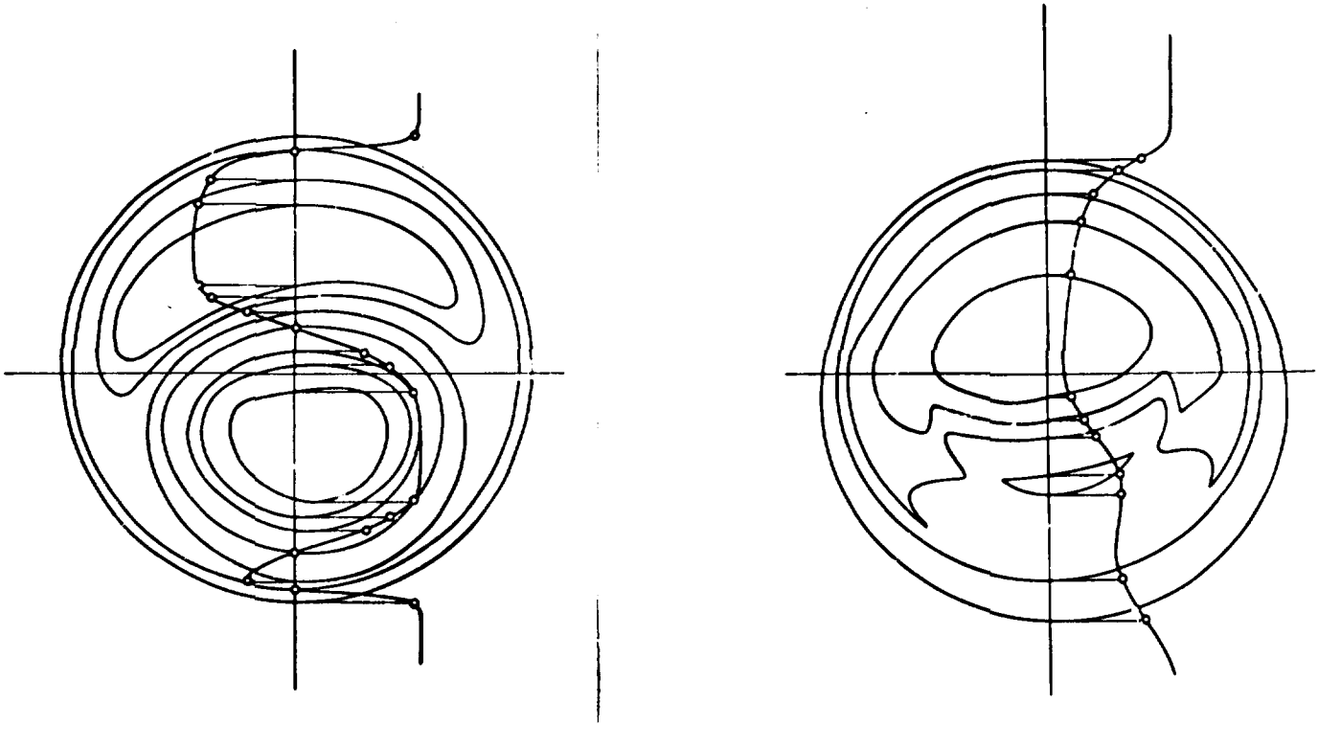

(a) x = 3.9 cm

(b) x = 24.3 cm

Figure 2. Contours of Constant Total Head in Wake without Dummy Strut (zero angle of attack). Core flow at first station is below centerline.

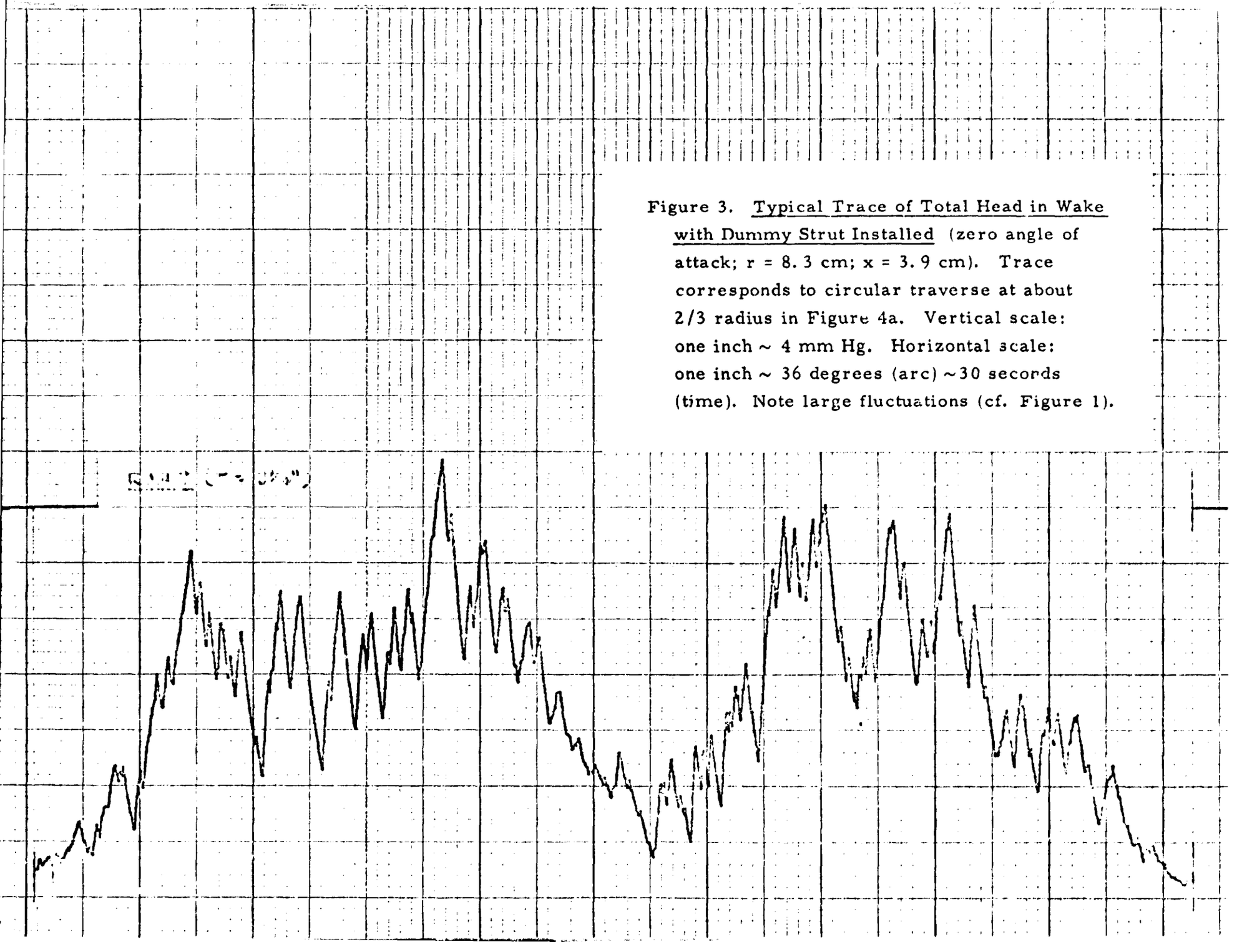

Figure 3. Typical Trace of Total Head in Wake with Dummy Strut Installed (zero angle of attack; r = 8.3 cm; x = 3.9 cm). Trace corresponds to circular traverse at about 2/3 radius in Figure 4a. Vertical scale: one inch ~ 4 mm Hg. Horizontal scale: one inch ~ 36 degrees (arc) ~30 seconds (time). Note large fluctuations (cf. Figure 1).

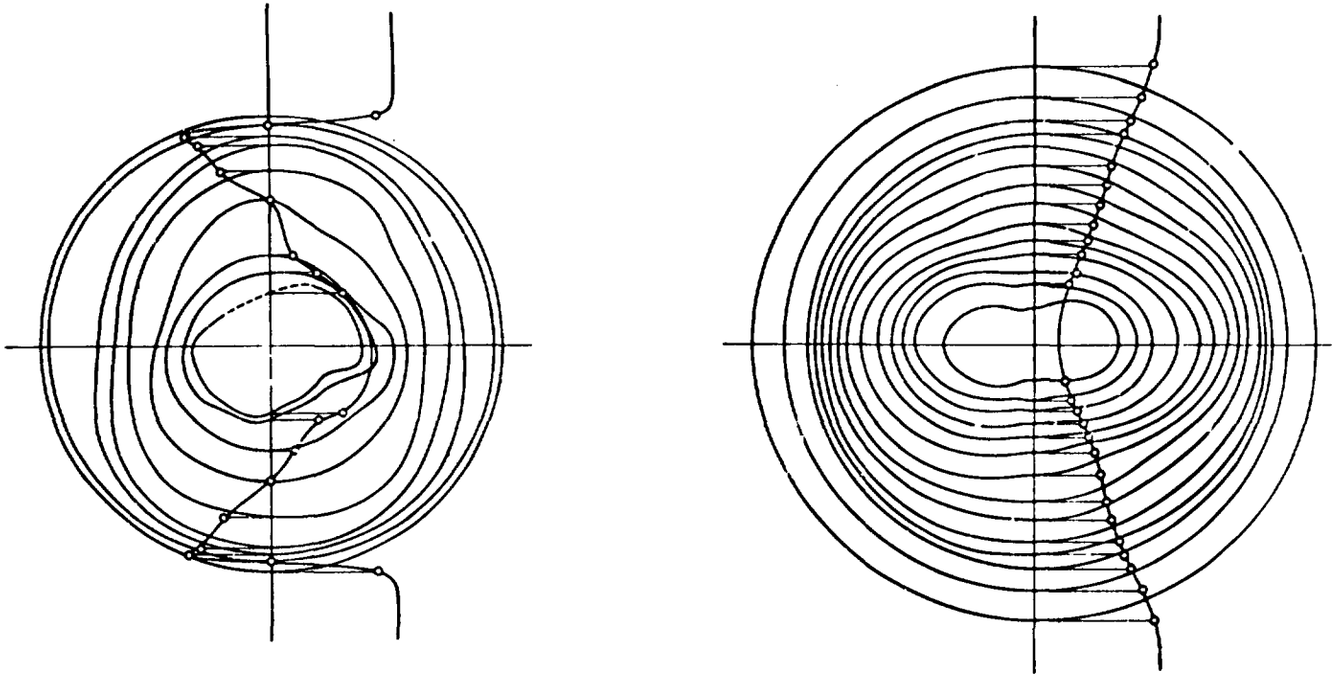

(a) x = 3.9 cm

(b) x = 24.3 cm

Figure 4. Contours of Constant Total Head in Wake with Dummy Strut Installed (zero angle of attack). Note absence of core flow even at first station.

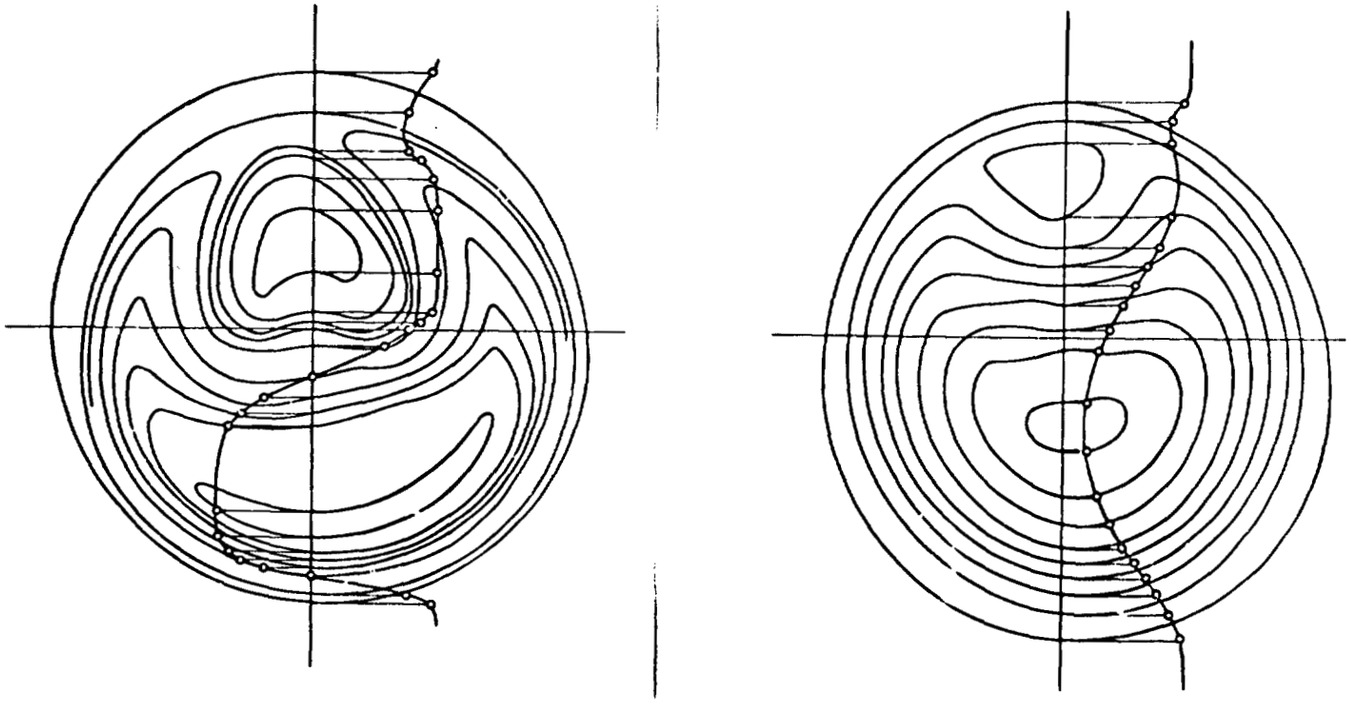

Figure 5. Contours of Constant Total Head in Wake with Ring Pitched Up Five Degrees. Core flow at first station is above centerline.

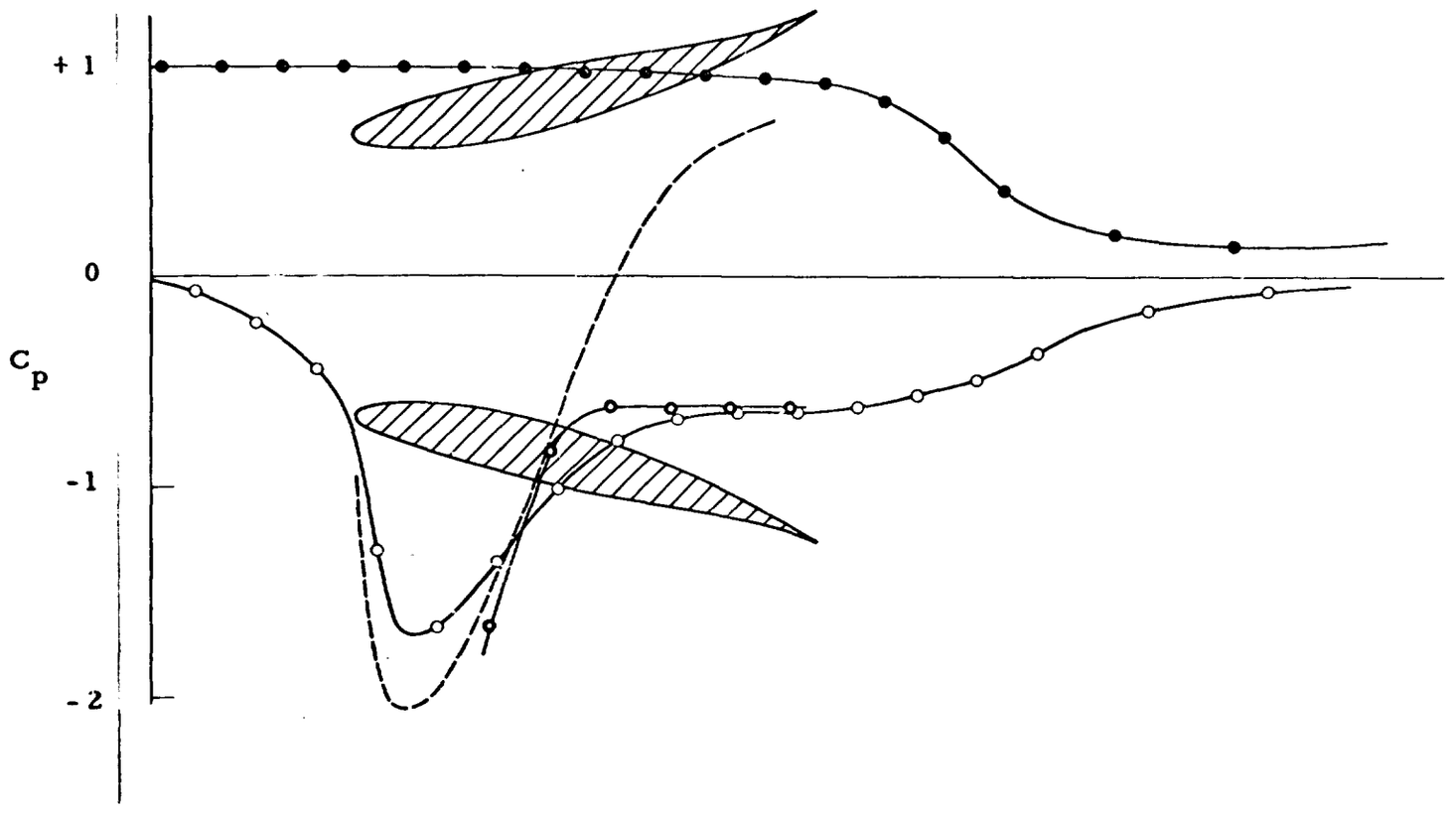

Figure 6. Variation of Static Pressure and Total Pressure along the Ring Axis and Elsewhere (flow from left to right; zero angle of attack; dummy strut installed). Notation: ● normalized total head on ring axis; O static pressure coefficient on ring axis; O static pressure coefficient extrapolated to aerofoil surface; — — — — — — static pressure coefficient computed for one-dimensional channel flow through ring.

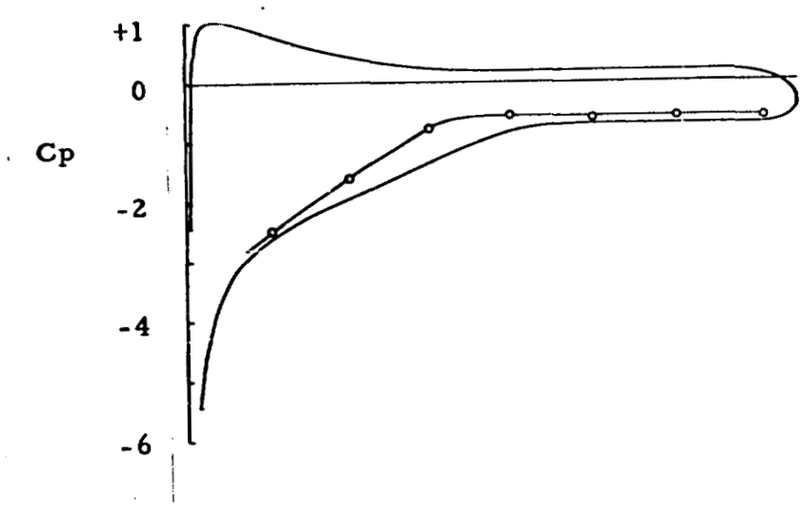

Figure 7. Surface Static-Pressure Coefficient in Separated Region Compared to Olson's Data (solid line) at 15 Degrees Angle of Attack.

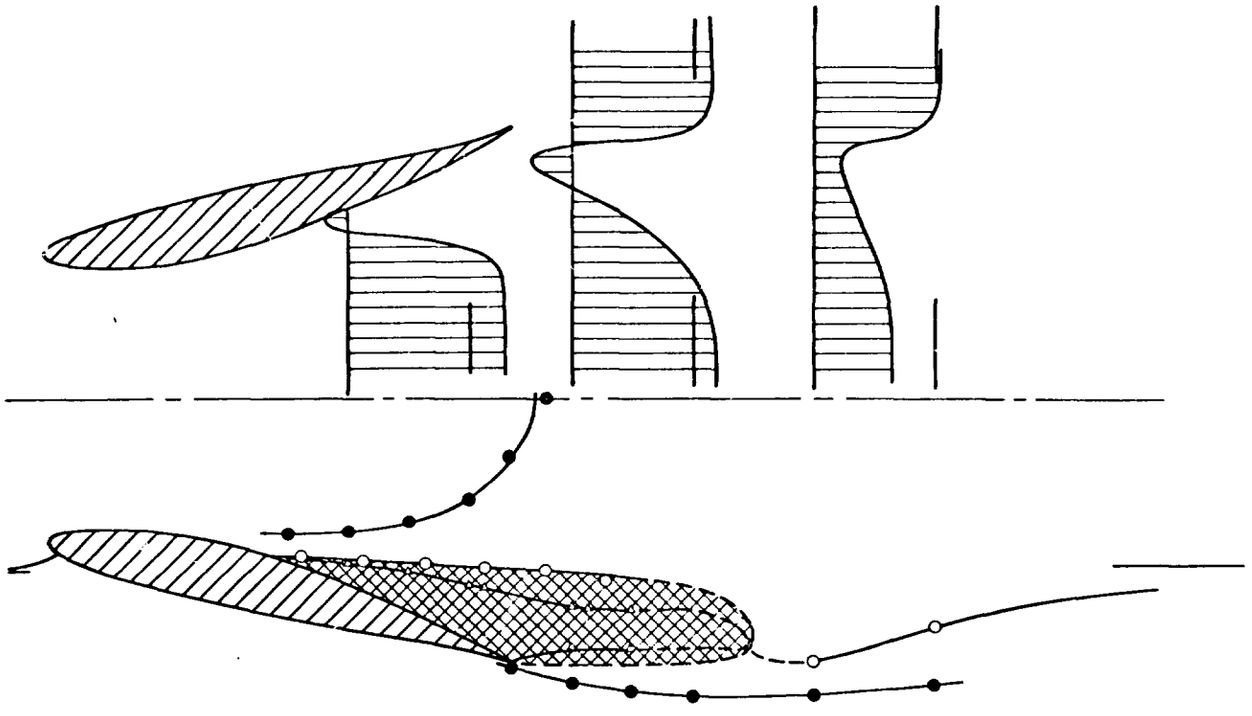

Figure 8. General Flow Pattern for Stalled Ring Aerofoil (flow from left to right; zero angle of attack; dummy strut installed; measurements in horizontal half-plane). Notation: ◐ approximate boundary of turbulent region (90 percent total head); ○ dividing mean streamline; △ line of zero mean velocity. Upper half of figure shows typical profiles of mean velocity scaled with velocity in external stream.